A Theoretical Study To Investigate D2DAR/D4DAR Selectivity: Receptor Modeling and Molecular Docking of Dopaminergic Ligands

Gabriella Ortore, Tiziano Tuccinardi, Simone Bertini, and Adriano Martinelli*

Dipartimento di Scienze Farmaceutiche, Università di Pisa, via Bonanno 6, 56126 Pisa, Italy

Received October 18, 2005

Molecular modeling methods have been applied to construct three-dimensional models for dopaminergic ligand complexes with D2 and D4 receptor subtypes (D2DAR and D4DAR), using the bovine rhodopsin crystal structure as a template for the modeling study. Different dopaminergic ligands, in particular the *N*-*n*-propyl-substituted 3-aryl- and 3-cyclohexylpiperidines, were docked into the D2DAR and the D4DAR, to evaluate the agreement between theoretical and experimental results as regards their D2/D4 selectivity. The different position of an aromatic region in the two receptors might explain the structural basis of this biological property.

Introduction

The neurotransmitter dopamine interacts with several receptors (DARs) that belong to the superfamily of G-protein-coupled receptors (GPCR) and plays a key role in the control of cognitive functions and emotional states.[1−3] Dopamine receptors can be divided into five different receptor subtypes and are further classified into two families,[4] D1-like (D1 and D5) and D2-like (D2, D3, and D4).[5−7] D2 and D3 receptors are the target of classic and some atypical neuroleptics, but according to neuropathological and genetic studies, selective dopamine D4 receptor agonists, partial agonists, or antagonists might be of interest for the treatment of neuropsychiatric disorders including mood disorders and Parkinson's disease.[8] Furthermore, a recent analysis has provided convincing evidence for the association between several allelic variations of the D4DAR with specific personality traits such as novelty seeking or impulsive, compulsive, and addictive behaviors, like susceptibility to drug abuse and compulsory gambling.[9] In addition, allelic variations of the D4DAR and D5DARs have been associated with attention deficit hyperactivity disorder (ADHD).[10] A general concern is that the altered behavior may result from a functional imbalance between the mesocortical and mesolimbic pathways, and compensation with stimulants or full agonists of a hypoactive pathway may lead to excessive stimulation of the other pathway. A therapeutic approach with partial agonists may solve the problem of imbalance between different dopaminergic pathways.[11,12]

By acting as a stimulant in those brain areas where the dopaminergic projection is hypofunctional, while preventing full activation of other brain regions that receive the hyperactive or normal projection, a partial agonist would adjust the balance between different anatomically and functionally distinct dopaminergic pathways. In this regard, the partial dopamine agonist aripiprazole has recently been proposed as the first member of a new class of antipsychotic drugs.[13]

This observation opens up the possibility that partial agonists selective for D4 receptors may have a therapeutic value also in ADHD and other hyperactivity disorders (HD). Highly D4-selective partial agonists with a 3-phenylpiperidine structure (PPEs) have been reported.[14,15] In particular, the *m*,*p*-dimethyl-substituted derivative, but also the mono methyl-substituted and the unsubstituted derivatives, had been reported to selectively activate the G proteins coupled to these receptors. These compounds were found to be more potent and selective than preclamol (3-PPP, Chart 1), reported as the first autoreceptor-selective agonist,[16] and indicated that the lack of polar substituents on the aryl leads to an increase in the D4DAR affinity. Therefore, it was possible to hypothesize that the aromatic moiety of PPE derivatives may interact with a lipophilic pocket present in the active site of the D4 DAR.[14,15]

Chart 1

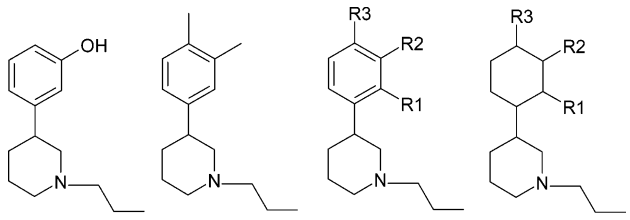

a: R1 = Me, R2 = H, R3 = H
b: R1 = H, R2 = Me, R3 = H
c: R1 = H, R2 = H, R3 = Me
d: R1 = H, R2 = H, R3 = H

Furthermore, with the aim of determining whether the nature of this interaction is aromatic or simply hydrophobic, some completely saturated analogues of PPE, the cyclohexylpiperidines (CHPEs), have been synthesized; these have been reported to be the first completely aliphatic compounds able to bind D4DARs selectively.[17]

To gain a greater understanding of the selectivity of PPEs, CHPEs, and other D4DAR agonists, we performed a modeling of D2 and D4 dopaminergic receptors and the docking of several ligands into these receptors, because accurate three-dimensional structural information about the dopamine receptors is not available and the structural basis of ligand binding and selectivity to the D4 receptor is not clear yet. Since rhodopsin and dopamine receptors belong to the same subfamily of the GPCR proteins,[18] the crystal structure of the rhodopsin was used as the template structure for modeling. The D2DAR and D4DAR models were then validated using available experimental information, like the substituted cysteine accessibility method results, mutational data, and the selectivity of known D2DAR and D4DAR ligands.

* Corresponding author. Tel: ++39-050-2219556. Fax: ++39-050-2219605. E-mail: marti@farm.unipi.it.

10.1021/jm051046b CCC: $33.50
Published on Web 01/17/2006

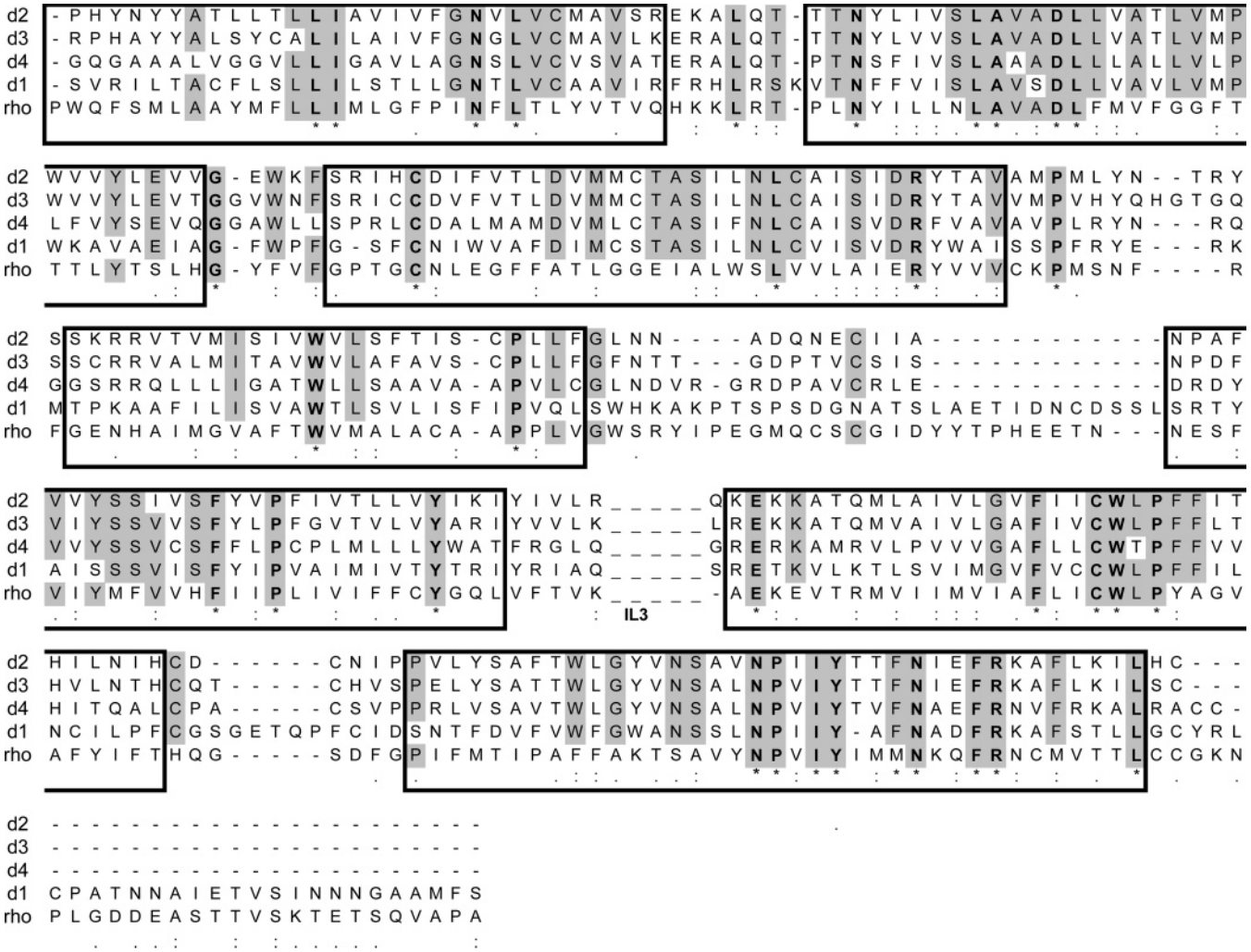

Figure 1. Alignment of the dopaminergic receptors and bovine rhodopsin amino acid sequences. The conserved residues are shaded in gray, in bold if strictly conserved. The other identical residues are indicated with "∗" and marked in gray in the TMs, while the conservatively replaceable residues are indicated with ":" and ".". The seven TM domains are boxed.

Results and Discussion

Molecular Modeling of D2DAR and D4DAR. We performed a modeling of the human D2DAR and D4DAR using the crystallographic structure of bovine rhodopsin[19] (RHO) as a template. The sequence identity between these dopaminergic receptors and RHO is less than 30% in the structurally conserved regions, but the presence in both D2DAR and D4DAR of a high percentage of the residues conserved within the GPCRs allows quite an accurate alignment, in good agreement with the findings of previous sequence analysis studies.[20,21] The sequence alignment between RHO and the dopaminergic receptors was generated through the program Clustal W,[22] with low gap penalties.

We considered the length of the secondary structure motifs derived from PSIPRED[23] prediction for D2DAR and D4DAR and from the experimental structure for the template, to avoid gaps and insertions in structured regions. We omitted the N-terminus and the intracellular loop IL3, because they are presumably remote from the binding site. Furthermore, the dopaminergic IL3 loop, much longer than that of bovine rhodopsin, was found to have no effect on ligand binding in previous studies on chimeric receptors.[24,25] Figure 1 shows that the highly conserved residues for all the dopaminergic receptors, and also the positions which appear to be important for the folding of the helices or for receptor activation, were aligned.

The loop regions show a significant sequence homology between the dopaminergic receptors and RHO, and the length of the dopaminergic loop sequences is comparable to that of the template, except for the loop IL3, which was omitted, and for the extracellular EL2 loop, which is connected to TM3 through a disulfide bridge[26] and thus conformationally restrained.

The alignment reported in Figure 1 was used to generate the three-dimensional models of D2DAR and D4DAR using the MODELLER program.[27] The model with the lowest energy and best geometry was chosen and refined by means of molecular mechanics (MM) and dynamics (MD) calculations and checked with PROCHECK[28] (see Experimental Section for details). The Ramachandran plot of the D2DAR model (Figure 2) revealed three residues in disallowed regions, all in the loop regions; for the D4DAR model there were five residues in disallowed regions, three localized in the loops and two in the TMs but far away from the binding site, Ala1.35(38) at the beginning of TM1 and Arg4.41(151) at the end of TM4.

The root-mean-square (rms) deviations along MD trajectories are given in Figure 2. The rms was calculated for structures along the trajectory relative to the one obtained through MODELLER, considering all the heavy atoms: the models of the D2DAR and D4DAR seem to reach an equilibrate structure.

The models of the D2DAR and D4DAR obtained in this way were finally compared with the experimental data reported in

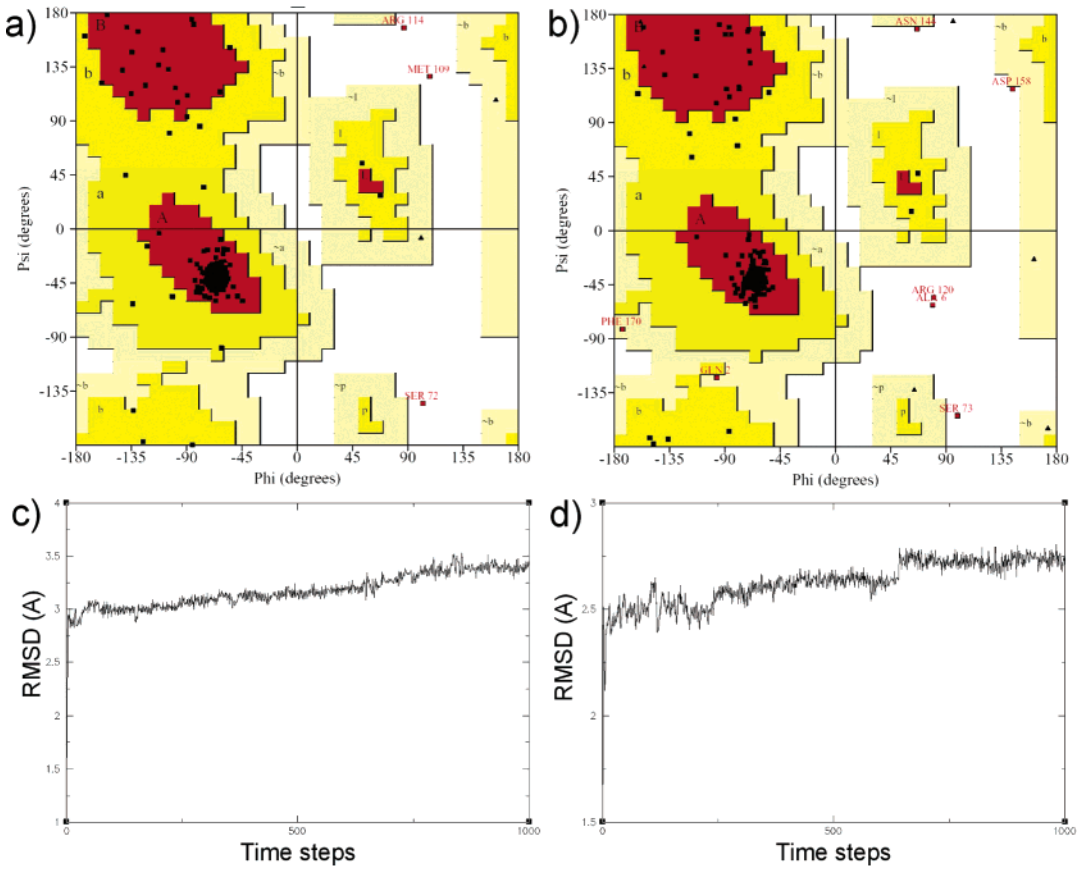

Figure 2. Ramachandran plot of the D2DAR (a) and D4DAR (b). The most favored regions are red, and additional allowed, generously allowed, and disallowed regions are indicated as yellow, light yellow, and white, respectively. The heavy atoms rmsd from the starting structures of the D2DAR (c) and D4DAR (d) as a function of simulation time at 300 K.

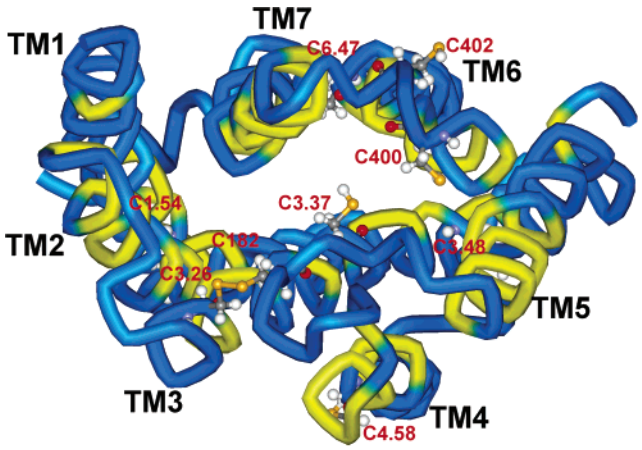

Figure 3. Position of the SCAM reactive residues and of the cysteines in our D2DAR model. The water exposed regions are yellow.

the literature for dopaminergic receptors, to validate their three-dimensional structures.

In particular, we considered the results of the substituted cysteine accessibility method (SCAM),[29−37] which provided a map of the D2DAR water-exposed residues on the basis of the reaction with MTS reagents and thus the residues that compose the surface of the binding site crevice. We found that the MTS-reactive residues of the D2DAR were situated in our model at the internal surface of the transmembranal crevice (see Figure 3), in the inner region of the receptor, or in the extracellular face of the receptor and thus exposed to the solvent, except for some residues of the TM5, which were not in agreement with the SCAM results. However, this discrepancy was detectable in the accessibility of 10 sequential cysteine substitution mutants, which was surprising and inconsistent with the helix folding of the TM5 and was probably due to the rapid move or conformational change of the helix that exposes different sets of residues to the binding site crevice at any given time.[31]

Another disagreement regarded Pro2.59(89); however, in opinion of the SCAM authors, this residue was too reactive, probably because of an altered structure of the P2.59C mutant with respect of the wild-type receptor.[34]

In agreement with Javitch et al.,[38] in our model (Figure 3) Cys3.26(107) and Cys182 formed a disulfide bond between TM3 and EL2 loop, Cys400 and Cys402 were extracellular, and among the five transmembrane cysteines, the only water-exposed one was Cys3.37(118).

Other experimental evidences, obtained by site-directed mutagenesis studies,[39,40] revealed six residues among the SCAM positive ones that could be related to D2DAR/D4DAR selectivity: Trp2.60(90), Val2.61(91), Leu2.64(94), Phe3.28(110), Val3.29(111), and Tyr7.35(408) in the D2DAR subtype, which are substituted by Leu2.60(90), Phe2.61(91), Ser2.64(94), Leu3.28(111), Met3.29(112) and Val7.35(430) in D4DAR.

Some mutations induced in highly preserved regions of biogenic amine receptors showed that Asp3.32, Ser5.43, Ser5.46, Phe6.51, and Phe6.52 are critical for the ligand affinity.[41−48] In particular, these data seem to suggest that (a) Asp3.32 forms a "salt bridge" with the aminic group of dopaminergic ligands, (b) there are hydrogen bonds between the meta-OH of dopamine and Ser5.43 and between the para-OH and Ser5.46, and (c) the residue Phe6.51 provides an aromatic stabilization of the dopamine ring.

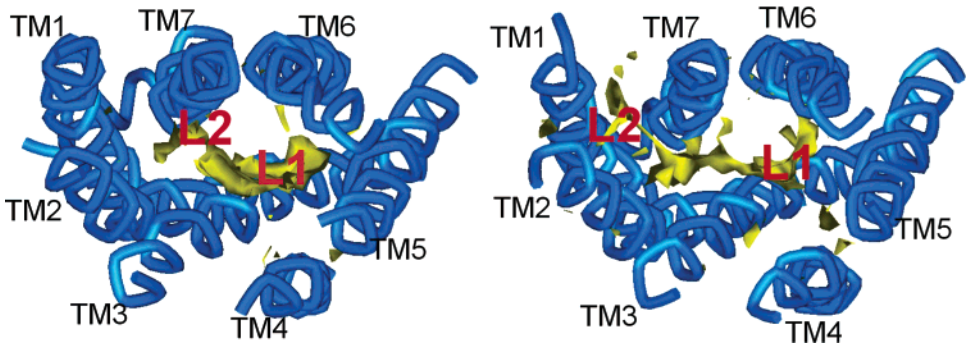

Figure 4. GRID maps of lipophilic regions in the hypothetical binding sites of D2DAR (left) and D4DAR (right).

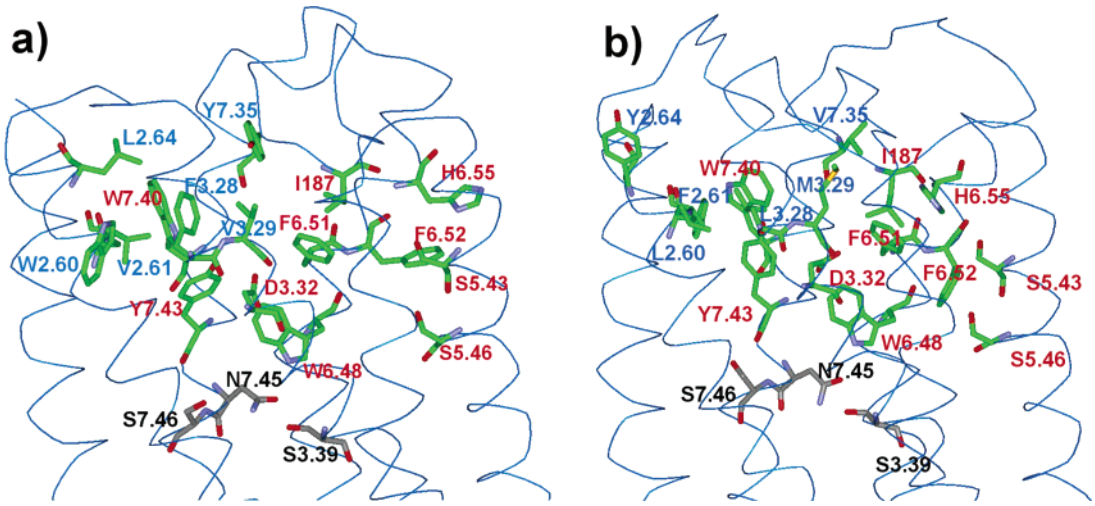

Figure 5. Subset of residues involved in the ligand binding at D2DAR (a) and D4DAR (b). The carbons of all the amino acids suggested by experimental data are green, and those suggested by this paper are gray. The blue labels indicate the residues responsible for the D2DAR/D4DAR selectivity; the red labels indicate the conserved amino acids considered critical for the biogenic amine receptors binding.

To verify that the three-dimensional structure of D2DAR and D4DAR allowed the interactions above cited, we introduced the biological ligand dopamine into the receptor models manually and found that its interactions with the receptor were in an agreement with the experimental results.

An analysis of the loop regions showed a marked conformational difference between the EL2 in the D2DAR and D4DAR receptor models. In both cases there was a disulfide bond between the TM3 and EL2 loop due to Cys3.26 and Cys182, but in the D4DAR this loop was constrained toward the TMs. The D4DAR EL2 loop was longer and more polar with respect to the D2DAR one, containing three arginine residues and a glutamate, which were not conserved in the D2DAR and were involved in various intramolecular interactions, for example that between Arg180 and Glu2.65 of the TM2.

Despite the different arrangement of the EL2 loop in the two receptors, in both cases only one residue was slightly inserted into the TMs region, Ile184 of D2DAR (Leu187 in D4DAR), in agreement with SCAM studies on the second extracellular loop of the D2DAR.[37]

A molecular interaction fields (MIFs) analysis was carried out using the GRID[49] program with the C1= probe, to identify the lipophilic regions in the hypothetical binding site of the D4DAR with respect to the D2DAR one.

The MIF map obtained is reported in Figure 4 and shows an analogous lipophilic region (L1) situated between TM3 and TM5, which is generated in the receptors by aromatic residues, and in particular by Trp6.48, Phe6.51, Phe6.52, and His6.55; furthermore, in both receptors there is another little lipophilic region (L2), which in the case of the D2DAR is situated near TM7 and is due to the residues Tyr7.35(408) and Phe3.28(110) (in the D4DAR they are a Val430 and Leu111), while in the case of the D4DAR, it shifts toward TM2 and is mainly generated by Phe2.61(91), a nonpreserved residue, together with Trp7.40(435) and Tyr7.43(438).

The hypothetical D2DAR binding site, which could be deduced through the site directed mutagenesis studies previously reported, is shown in Figure 5.

This region includes all the residues that could be related to D2DAR/D4DAR selectivity[47,48] or which are critical for the ligand affinity in the biogenic amine receptors.[50] In agreement with the data reported in the literature, we inserted the dopamine into the D2DAR and D4DAR binding sites, with the catecholic group pointing toward the TM5 serines, the para-OH hydrogen bonded to Ser5.46 and the meta-OH to Ser5.43, and the protonated nitrogen bonded to Asp3.32. The complexes with the biological ligand were refined through MD simulations, using the procedure described in the Experimental Section, with the aim of verifing that the conformational space of our receptor models bound to the dopamine were satisfactory to stabilize the ligand and validate the experimental data.

The final D2DAR− and D4DAR−dopamine complexes were very similar: the polar bonds with Asp3.32 and the TM5 serines were still present after the MD calculations (see Table 2), and the residues' arrangement of the binding site allowed a good interaction between the aromatic moiety of dopamine and Trp6.48, Phe6.51, Phe6.52, and His6.55, as in the predicted binding model.[50]

Table 1. Structure and Binding Data of the Ligands Considered in This Study

COMPOUND	Ki D2 (nM)	Ki D4 (nM)
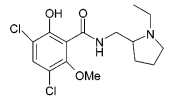 **1**	5,10[a]	2923[a]
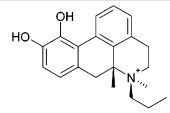 **2**	9,6[b]	0,6[b]
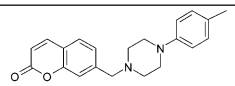 **3**	5700[c]	17[c]
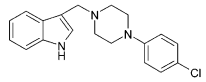 **4**	960[d]	0,45[d]
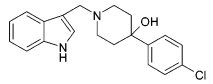 **5**	2,90[d]	230[d]
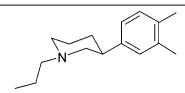 **6**	5000[e]	23[e]
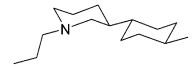 **7**	64000[e]	4[e]

[a] Competition of specific binding of 0.2 nM [^{3}H]spiperone to CHO K1 cells stably transfected with the human D2 and D4 receptor.[52] [b] As in footnote *a*.[53] [c] As in footnote *a*.[54] [d] Competition of specific binding of 0.2 nM [^{3}H]spiperone to clonal cells stably transfected with the human D2 and D4 receptor. Cell lines used were hD2 CHO and hD4 HEK.[55] [e] Radioreceptor binding studies with [^{3}H]-YM-09-151-2 performed in membrane preparations from bovine retina and striatum.[15,17]

Docking and Modeling of Ligand−Receptor Complexes. We used the molecular models of D2DAR−dopamine and D4DAR−dopamine, although derived from a modeling procedure, for automated docking. We used the AUTODOCK[51] program to produce the more plausible dopaminergic complexes for the ligand reported in Table 1.

We generated the AUTODOCK grid cage around the Asp3.32 as a center, in such a way as to enclose all the residues suggested by literature[47,48,50] (reported in green in Figure 5), and also another region within a range of 11 Å from Asp3.32 capable of interaction with the polar moiety of the ligands instead of the TM5 serines, due to Asn7.45, Ser7.46, and Ser3.39, which was already considered as part of the D2DAR binding site in a previous modeling study[21] (shown in gray in Figure 5). This wide binding site allowed more freedom in the orientation of the bulkiest dopaminergic ligands considered in this work (see Table 1), which could be inserted "across" the receptor crevice, in a space of about 20 Å between TM2 and TM5, or in the middle of the receptor channel, parallel to the helices rather then across the cavity, in a region delimited from TM2, TM3, TM6, and TM7 and quite distant from TM5. In this way, we considered a wide grid cage which allowed a good insertion of some ligands also without the hypothesized interactions with the TM5 serines, which were decisive for the binding of many dopaminergic ligands, for example dopamine, *N*-propylnorapomorphine (NPA), and raclopride, and less significant for others, like haloperidol, which is structurally more similar to compounds **3**−**5**.[42,44] There is no experimental evidence for a recurrent binding between the non-cathecholic scaffolds and the Ser5.43 and Ser5.46.

In a grid cage of 80 × 50 × 30 points we performed an automated docking of the biological ligand dopamine, to test the AUTODOCK procedure (see Experimental Section) and its ability to reproduce the binding geometry of dopamine obtained by means of the molecular dynamics procedure. AUTODOCK found an analogous binding mode corresponding to the one obtained by manual docking, with a rms deviation between the lowest energy docked conformation and the dopamine manually docked one of 0.3 Å (rms evaluated over all the heavy atoms of the ligand). Thus, we carried out the automated docking of raclopride[56] (**1**), *N*-propylnorapomorphine[45] (**2**), the phenylpiperazine chromen-2-one **3**,[54] L-741,626[57] (**4**), L-745,870[57] (**5**), the phenylpiperidine dimethyl-substituted **6**,[14,15] and the 4-methylcyclohexylpiperidine **7**[14,15] using the same docking protocol.

Because the results of the AUTODOCK calculations are different depending on the starting point coordinates of the ligand, for some compounds we used two starting orientations. The default settings of AUTODOCK consider the initial position of the ligand as RANDOM, and the docking procedure was free of constraints and therefore it was possible to explore all the space of the grid cage. The starting positions of all the

Table 2. Distance in Å between Ligands (columns) and Residues of the Binding Site (rows) of D2DAR and D4DAR, in a Range of about 5 Å[a]

	D2DAR									D4DAR							
residue	Dopa	**1**	**2**	**3**	**4**	**5**	**6**	**7**	residue	Dopa	**1**	**2**	**3**	**4**	**5**	**6**	**7**
W 2.60	−	−	−	5.1	−	−	−	−	L 2.60	−	−	−	−	−	−	−	−
V 2.61	−	−	−	−	−	−	−	−	F 2.61	−	−	−	4.0	4.1	−	4.4	4.5
L 2.64	−	−	−	−	4.5	−	−	−	S 2.64	−	−	−	−	−	−	−	−
F 3.28	−	4.6	4.7	4.4	3.2	5.0	4.4	4.7	L 3.28	−	−	−	−	−	4.1	4.8	4.8
V 3.29	−	4.7	5.1	3.6	3.6	−	4.1	4.8	M 3.29	−	−	−	4.7	5.0	4.4	5.0	5.0
D 3.32	2.7	2.7	2.7	3.0	2.5	3.0	2.7	2.8	D 3.32	2.7	2.9	2.7	2.7	2.7	2.9	2.8	2.7
T 3.37	4.1	2.9	4.3	−	−	−	−	−	T 3.37	4.5	−	−	4.3	−	−	−	−
S 3.39	−	−	−	−	−	2.8	−	−	S 3.39	−	−	−	−	−	−	−	−
I 184	5.0	4.7	5.1	5.0	5.0	−	−	−	I 184	4.9	4.6	4.9	4.6	−	5.1	4.3	4.3
S 5.43	3.1	−	3.6	4.1	4.0	−	−	−	S 5.43	3.0	−	2.9	3.5	3.2	−	−	−
S 5.46	2.7	4.3	4.1	4.2	−	−	−	−	S 5.46	2.7	−	3.6	3.4	4.2	−	−	−
W 6.48	3.5	4.6	4.1	−	−	−	5.2	4.9	W 6.48	3.4	5.0	4.5	4.8	5.1	−	−	−
F 6.51	4.2	4.7	3.9	4.1	4.4	4.0	4.3	4.5	F 6.51	4.4	4.5	4.0	4.0	4.1	4.6	4.8	4.7
F 6.52	−	−	−	−	−	−	−	−	F 6.52	−	−	4.5	−	−	−	−	−
H 6.55	−	−	−	−	−	−	−	−	H 6.55	4.8	−	4.8	4.6	4.4	−	−	−
Y 7.35	−	−	−	4.1	3.7	−	4.9	5.0	V 7.35	−	−	−	−	−	−	−	−
T 7.39	−	4.7	5.1	3.7	3.7	4.8	4.1	4.6	T 7.39	−	5.0	5.1	3.2	4.5	3.7	3.6	4.4
W 7.40	−	−	−	5.0	4.8	−	4.4	5.0	W 7.40	−	−	−	3.6	5.2	4.8	4.8	4.6
Y 7.43	−	4.8	4.5	−	5.0	4.0	4.8	−	Y 7.43	−	5.0	4.8	3.2	4.0	5.0	4.9	4.4

[a] The measures are relative to the closest atom of the ligand, the center of the ring if the closest part of the ligand is an aromatic group and the heteroatom if it is involved in a hydrogen bond.

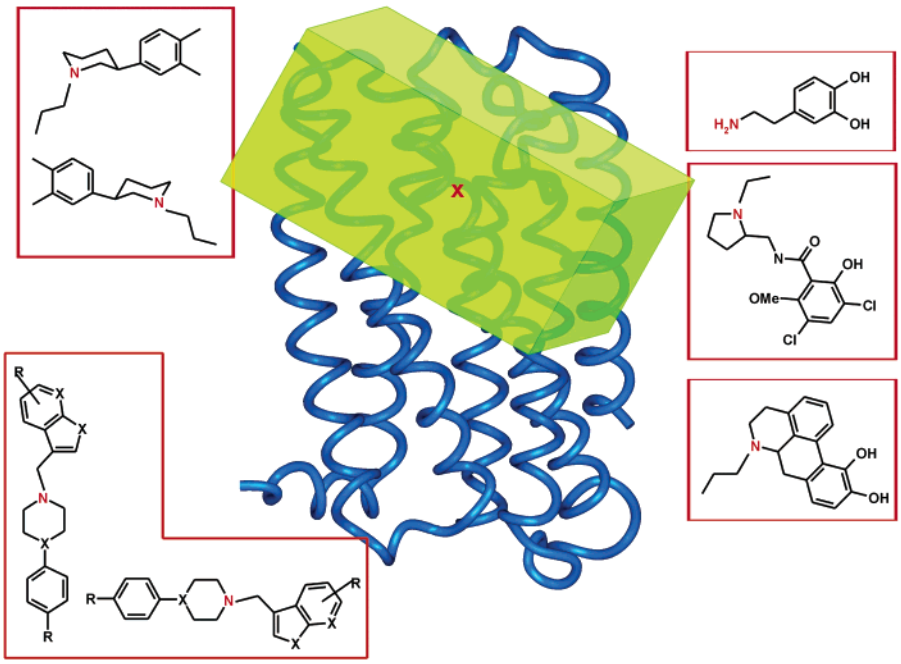

Figure 6. Starting orientations for the automated docking of the ligands in the AUTODOCK grid cage. The ligands were placed into the receptors in such a way as to allow the interaction between Asp3.32 (the red cross in the grid) and the protonate N of the ligands (red). Two orientations were considered for the compounds **3**−**7** and only one for dopamine, **1**, and **2**.

compounds provided a bond distance between Asp3.32, represented in Figure 6 by a red cross, and the protonate nitrogen of the ligands.

For raclopride and NPA, we used only one starting position in the same region as for dopamine, because, like the biological ligand, these compounds seem to be influenced by the mutation of the TM5 serines.

For compounds **3**−**5**, there were no mutagenesis results regarding ligand binding; thus, we considered both the possible starting orientations showed in Figure 6: the first, *across* the receptor crevice, from TM2 to TM5, the second, *along* the cavity and parallel to the TMs.

The new compounds **6** and **7** are very different with respect to the traditional selective D4DAR ligands and are completely unable to bind the serines because of their lipophilic structure. Thus, the only hypothesis about their position in the receptors regarded the ionic bond between Asp3.32 and the piperidine nitrogen; for these compounds we used as starting positions the same as for dopamine or the symmetric orientation with respect to TM3, between Asp3.32 and Phe2.61 (see Figure 6).

The docking results were analyzed on the basis of the complexes binding energies and of the population clusters, choosing the first orientation of the best-populated cluster. For compounds **3**−**7**, we considered the two best-populated clusters obtained from the docking performed with the two starting orientations and choose the best-populated one, but if the populations of the two clusters were comparable, we choose the one with a lower average docking energy.

The best complex obtained for each ligand was finally refined through 1000 ps of MD (see Experimental Section).

Analysis of the Docking Results. The orientation of dopamine is very similar in the two receptors: in both the complexes an ionic interaction with Asp3.32 and two strong hydrogen bonds with Ser5.43 and Ser5.46 are present, and the cathecolic ring is surrounded by the aromatic residues Trp6.48, Phe6.51, Phe6.52, and His6.55 described in the literature. The only difference concerns His6.55, which in D4DAR greatly stabilizes the dopamine, whereas in the D2DAR it turns away (the distance between the ring centers of His6.55 and dopamine is 6 Å). The EL2 loop region is near the binding site, but the closest residue in the D2DAR, Ile184, which correspond to Leu187 in D4DAR, has a distance of 5 Å from the cathecolic ring (see Figure 7 and Table 2).

Raclopride (**1**),[56] a selective ligand for D2DAR, occupies the same position in both the dopaminergic subtypes, but in the D2DAR the ligand is involved in a close network of hydrogen bonds [Asp3.32(114)−aminic N, Cys3.36(118)−amidic N, Thr3.37(119)−phenolic OH, Thr3.37(119)−Ser5.46(197)], which do not include Ser5.43. Furthermore, the aliphatic portion of raclopride lies in a lipophilic pocket that points toward the L2 region, where the presence of Phe3.28(110) and Tyr7.35(408) at a distance of 4.7 and 6 Å from the ligand, instead of Leu111 and Val430 of the D4DAR, allows a better lipophilic interaction. These results were in agreement with the experimental data, which show that the mutation of Ser5.43(194) with alanine in the D2DAR has a poor influence on the binding, while the S5.46A leads to a decrease in affinity, which could be due to a loss of interaction with this serine.[44]

For NPA (**2**)[45] the final geometry is the same as that of dopamine. Also in this case, a better lipophilic stabilization of the ligand in the D4DAR might explain a slightly selectivity for this receptor.

The phenylpiperazine chromen-2-one **3**[54] has a scaffold typical of the D4DAR selective ligands, similar to that of haloperidol. The quite long and semirigid structure allows a good insertion of the ligand both *across* the receptors, in the region delimited by all the residues suggested by SCAM and mutagenesis studies, and in the *along* binding mode, without any interaction with the TM5 serines. On the other hand, there was not any experimental data suggesting that these compounds can interact with these residues.

Thus, we tried these two starting positions for the docking of compound **3**, and the first orientation of the best populated of all the clusters shows very clearly the trend of the phenyl ring to interact with the L2 region of the D2DAR, in particular with Phe3.28(110) and Tyr7.35(408), also turning the chrome-

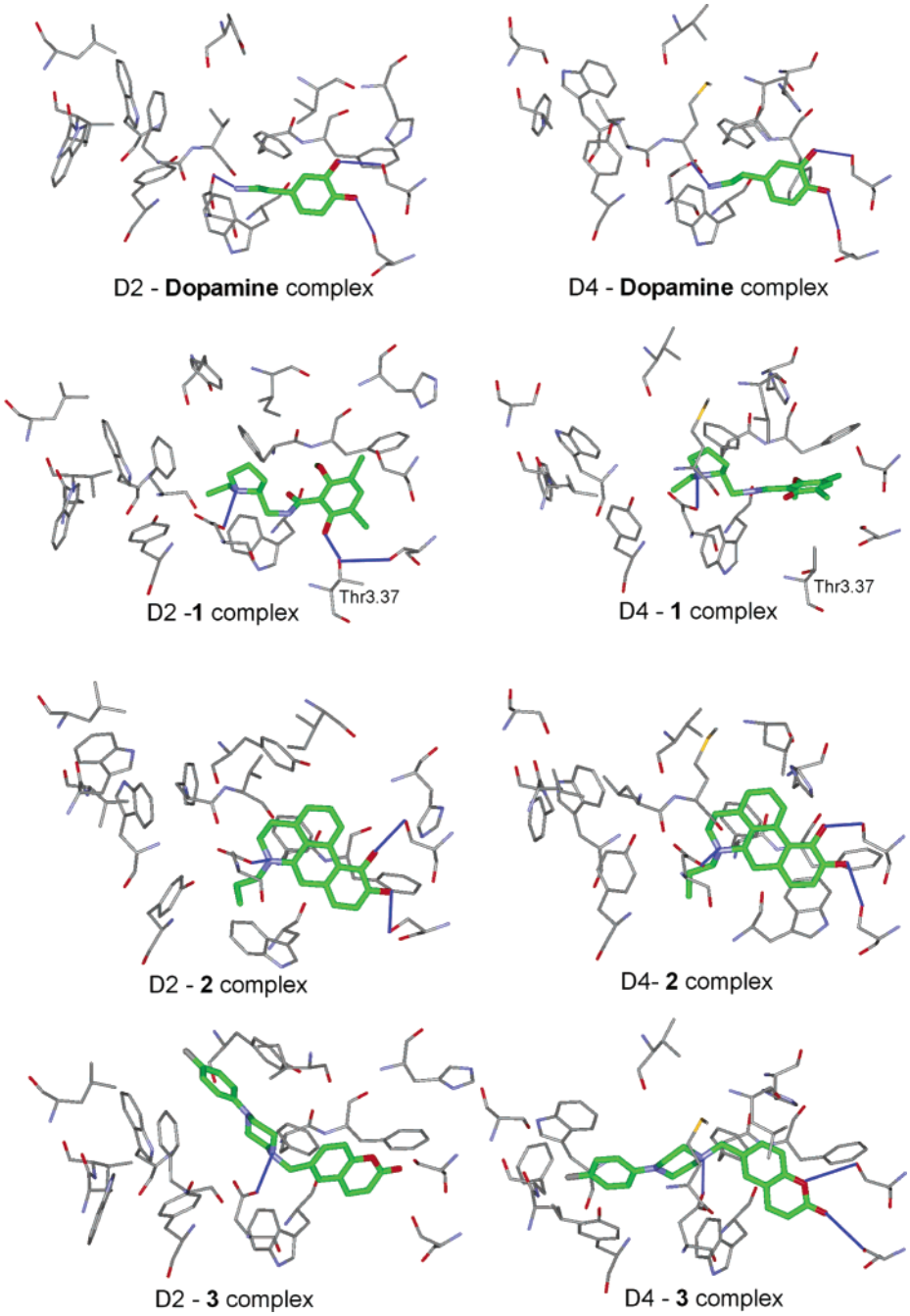

Figure 7. View of the interaction between D2DAR and D4DAR binding sites and the ligands dopamine, **1**, **2**, and **3**.

none upward and losing the interaction with the TM5 serines. In the D4DAR, instead, the main interaction of the chlorophenyl ring is with Phe2.61(91) and Tyr7.43(438), and the ligand conformation allows a strong interaction with Ser5.43(197) and Ser5.46(200).

The same trend regards compound **4**, L-745,870,[57] another D4DAR selective partial agonist[58] that has a very similar structure to the previous chromenone and shows an analogous arrangement in the receptors (Figure 8). Also in this case there is a ionic bond Asp3.32(115)−protonate N, the hydrogen bonds between the azaindolic ring and the TM5 serines, and the lipophilic interaction between the chlorophenyl ring and Phe2.61-(91) (as hypothesized for the analogue L-750667 through site-directed mutagenesis studies[59]) at the L2 region of the D4DAR. In the D2DAR, the interaction with the L2 domain shifts the ligand toward the extracellular space, moving away from Ser5.43(194) and Ser5.46(197).

The L-741,626 (**5**)[57] presents a scaffold equivalent to that of L-745,870, analogous to haloperidol but with a D2DAR affinity about 10-fold higher than that of the D4DAR. In this case, the presence of the −OH on the piperidine ring changes the trend of the AUTODOCK results, and the best orientation was *along* the receptor. In the D2DAR, this position was strongly stabilized by many polar interactions [ionic bond Asp3.32(114)−protonated N, hydrogen bonds between Ser3.39(121)−piperidine OH and Thr7.39(412)−indolic NH] and by the insertion of the indolic ring between Phe7.38(411) and Phe6.51(389), pointing toward the L2 region. In the D4DAR, the ligand loses all these polar interactions and lacks the same aromatic stabilization in the upper region, because of the presence of Leu3.28(111) and Val7.35(430) instead of Phe110 and Tyr408.

The dimethyl-substituted phenylpiperidine **6**[14,15] is very different with respect to the traditional selective D4DAR ligands, like **3** and **5**: it is smaller and more lipophilic and does not fill

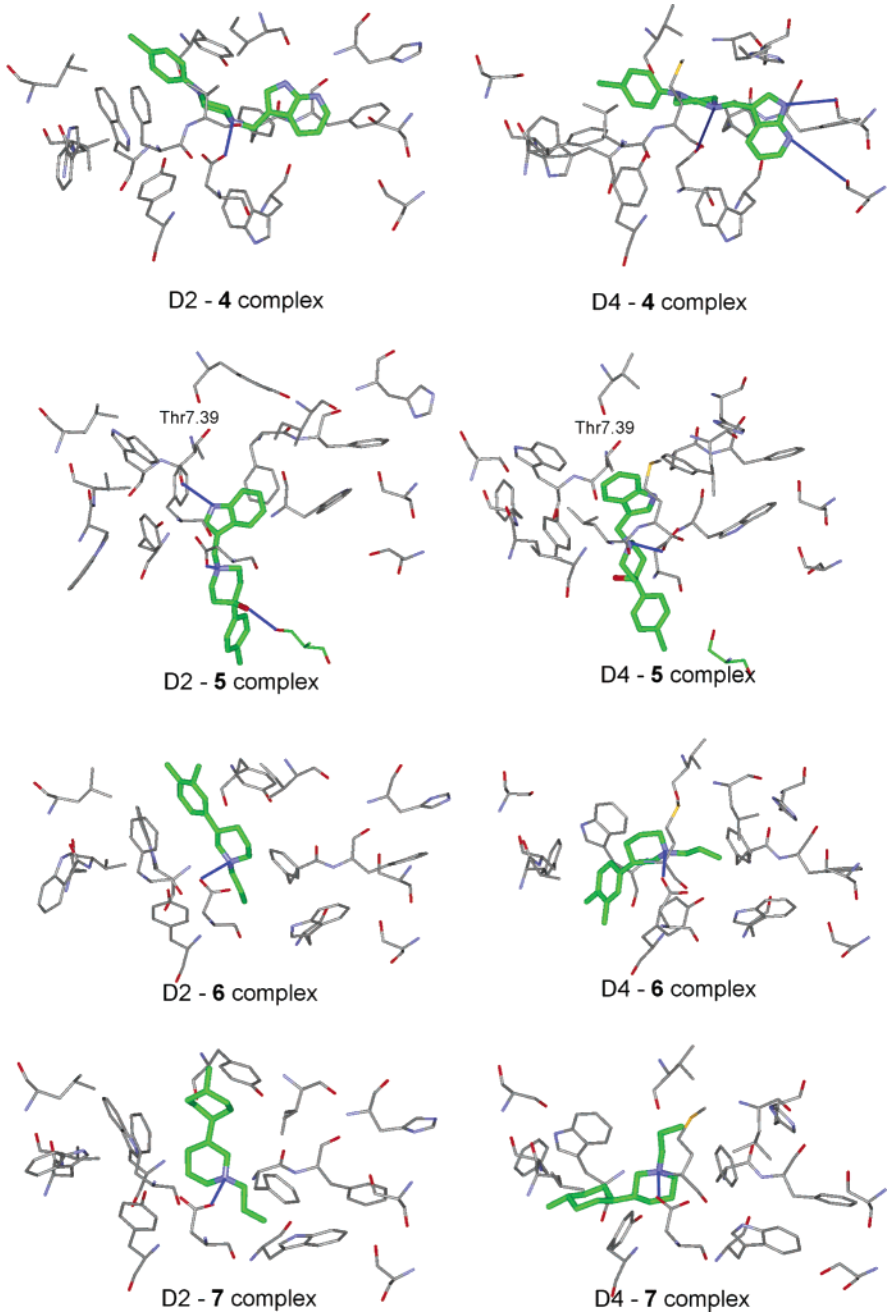

Figure 8. View of the interaction between D2DAR and D4DAR binding sites and the ligands **4**−**7**.

the channel of the dopaminergic receptor. The main interaction hypothesized also for these compounds was the ionic bond between the piperidinic nitrogen and Asp3.32.

The strong selectivity of this compounds for the D4DAR suggested that it could be due to an interaction with the L2 region of this receptor, which was considered to be decisive for D2DAR/D4DAR selectivity.

The automated docking which was performed by considering two starting-point orientations, as above-described, showed that the most favorable orientation is the one indicated in Figure 8, i.e., roughly symmetric with respect to the dopamine one in both receptors. Despite its small dimensions, this molecule showed the same trend as the other bulky D4DAR selective ligands: compound **6** interacts with Asp3.32 in both the dopaminergic subtypes, but in the D2DAR the interaction of the lipophilic part of the ligand with the L2 domain shifts the compound toward the extracellular region. In the D4DAR, the phenylpiperidine is positioned in the inner part of the receptors because of the lipophilic stabilization due to the nonpreserved Phe2.61(91) and to Tyr7.43(438).

Very similarly to PPEs, their aliphatic derivatives, the CHPEs, and in particular the 4-methyl-substituted derivative **7**,[14,15] show a different arrangement in the D4DAR with respect to the D2DAR. A deep insertion into the transmembrane domain of the D4DAR is allowed also for this ligand, due to the favorable interaction with the L2 region, while in the D2DAR compound **7** shifts toward the nonconserved Tyr7.35(408), assuming a very unfavorable conformation of the cyclohexyl ring.

Conclusions

The molecular models of D2DAR and D4DAR were built to explore the putative binding sites of these receptors and to explain the different selectivity of the considered ligands despite their great structural differences.

The models showed that the binding pocket in both the D2DAR and the D4DAR is situated between residue 2.61 (a

valine in the D2DAR and a phenylalanine in the D4DAR) and serines 5.43 and 5.46.

The protonated aminic group commonly present in a dopaminergic ligand binds the Asp3.32; therefore, this residue is generally considered to be mainly responsible for the affinity of a ligand for both receptors.

The main difference between the two receptors seems to be due to the lipophilic L2 region in the binding site (Figure 4), which is situated in a different position in the two receptors: in the D2DAR it is due to Phe3.28(110) and Tyr7.35(408), corresponding in the D4DAR to Val3.28(111) and Val7.35 (430), while in the D4DAR the L2 region is due to Phe2.61-(91), corresponding in the D2DAR to Val2.61(91).

Therefore, the selectivity toward the D4DAR with respect to the D2DAR could be due to the ability of a D4DAR-selective ligand to interact with the region near Phe2.61(91) of the lipophilic region L2 of the D4DAR and this is confirmed by mutagenesis data, which indicated that this residue is important for the binding to D4DAR.

Some authors have hypothesized that the selectivity for D4DAR might be explained on the basis of the presence of a dense cluster of aromatic residues in the D2DAR within TM2−TM3−TM7 near the extracellular side [Trp2.60(90), Phe3.28-(110), Tyr7.35(408) and Phe7.38(411)], which could act as a barrier preventing binding of bulky ligands. This hypothesis was in agreement with the bulky structure of the more classical D4DAR selective agents such as **3** and **4** but seems to be unable to explain the affinity of small molecules for the D4 subtype.

The results of this study seem to suggest that the aromatic cluster of the D2DAR, which in our model is localized about in the same region of the previously quoted one, has a stabilizing effect rather than a barrier role.

Raclopride (**2**) has a very small lipophilic portion close to the protonated nitrogen, which can interact with the L2 region of the D2DAR, and this could be the reason for its selectivity for this receptor.

D4DAR-selective compounds **3** and **4**, which are quite big and lipophilic, can efficiently fill the whole cavity of the D4DAR, between TM2 and TM5, and their aromatic substituents allow an effective interaction with the L2 region. However, compound **5**, despite its structural similarity to **4**, is a D2DAR-selective ligand because it is stabilized by the L2 region of the D2DAR, while it is unable to interact with the L2 region of the D4DAR, due to the presence of a hydroxyl group: it prefers another binding mode with respect to compounds **3** and **4**.

PPE, **6**, and CHPE, **7**, are small lipophilic dopaminergic ligands, very different with respect to the traditional selective D4DAR ligands. They are unable to fill the whole binding site, but they have a structure in which there is the right distance between the aminic group and the lipophilic portion to optimally occupy the region between the L2 region and Asp3.32 of the D4DAR, while this distance is too great to interact effectively with the L2 region of the D2DAR.

They engage a strong interaction with the L2 region of the D4DAR and in particular with Phe2.61(91): compound **6**, could suggest that the nature of this interaction should be of an aromatic $\pi-\pi$ stacking type, but the analogue binding mode of compound **7** and the favorable effect of the Phe2.61 on the stabilization of its cyclohexyl ring rather indicates that also another lipophilic group is able to efficiently interact with the L2 region of D4DAR.

Therefore, a new basis for designing new selective D4 ligands could be the difference of the distance L2 region−Asp3.32 between the D4DAR and the D2DAR rather than the molecular hindrance of the ligands.

Experimental Section

Dopamine Receptors Modeling. The 3D X-ray crystallographic structure of bovine rhodopsin registered in the Protein Data Bank[60] (1F88)[19] was used as a direct template to construct the dopaminergic receptors, while all the primary sequences were retrieved from the SWISS−PROT[61] protein sequence database. The sequential alignment of rhodopsin and the human dopaminergic D2DAR and D4DAR was performed by means of CLUSTAL W,[22] using the Blosum series as a matrix, with a gap open penalty of 10 and a gap extension penalty of 0.05. The Psipred program[23] was used in order to verify the presence of α-helices in our TM sequence hypothesis. We omitted the IL3 loop in the sequences alignment, because it is not decisive for ligand binding. For the IL1, EL1, and EL3 loops we used the rhodopsin crystal structure as a template because there was a sequence identity of about 30%. The alignment of the EL2 loop on the rhodopsine one was not so good, but nevertheless, we used this structure as starting point for the molecular dynamics simulation because the Cys3.26−Cys182 disulfide bridge connecting the EL2 loop with TM3, which was the main structural requirement, gave a strong limitation to the conformational space. The alignment was in a good agreement with previous works,[20,21] which had taken into consideration several TM receptor sequences for alignment.

To refer to specific amino acids sequences, the numbering system suggested by Ballesteros and Weinstein is used.[62] The most highly conserved residue in each transmembrane helix (TMH) is assigned a value of 0.50 and this number is preceded by the TMH number and followed in parentheses by the sequence number. The other residues in the helix are given a locant value relative to this. The 3D models of D2DAR and D4DAR were constructed using the MODELLER program,[27] on the basis of the alignment obtained from CLUSTAL W and Psipred analysis. The helices ends were capped with an acetyl group at the N-terminus and with an *N*-methyl group at the C-terminus. The whole system was then subjected to preliminary minimization followed by 40 ps of heating and 1000 ps of MD, using a constraint with a decreasing force constant (10−0.1 kcal/mol) on the Calfa to avoid changes in the general fold. All the molecular mechanics and molecular dynamics calculations were performed by means of the SANDER program of the AMBER8 suite.[63] In molecular mechanics calculations (MM) the minimization algorithms were steepest descent followed by conjugated gradient until a convergence value of 0.005 kcal/Å·mol; in molecular dynamics simulations, the temperature was set at 300 K and the time step was 1 fs. We used the SHAKE algorithm[64] to constrain the hydrogen bonds, with boundary conditions of constant volume and a nonbond cutoff distance of 12 Å. The average structure from the last 200 ps trajectory of MD was minimized until a rms of 0.005 kcal/Å·mol was reached. The stereochemical quality of the resulting protein structures was evaluated by inspection of the ψ/φ Ramachandran plot obtained from PROCHECK analysis.[28] The MD snapshots were obtained through the PTRAJ module of AMBER8.

Modeling of D2DAR− and D4DAR−Dopamine Complexes. The dopamine was build in trans-β-rotamer conformation using the Maestro program[65] and then was minimized through the conjugated gradient method using MMFFs force field and a distance-dependent dielectric constant of 4.0, until a convergence value of 0.005 kcal/Å·mol.

Partial atomic charges from the AM1-BCC (bond charge correction) method[66] and AMBER atom types were assigned using the ANTECHAMBER module[67] of AMBER8.

Dopamine was manually docked into both receptors by maximizing the interactions hypothesized on the basis of the experimental studies reported in the literature: the positively charged nitrogen with Asp3.32, the meta OH of the cathecolic nucleus with Ser5.43, and the para OH with Ser5.46. The resulting complexes were submitted to the same protocol of molecular dynamics previously

described. Besides the slight constraints on the Cα, we applied a constraint on the main ligand−receptor interactions with a decreasing force constant (30, 20, 10, 1 kcal/mol) on the first 800 ps of MD, leaving the ligand free in the last 200 steps. Also in this case, a minimization was applied to the structure obtained as the average of the last 200 ps.

Docking Procedure. The ligands were submitted to a conformational search of 1000 steps through MACROMODEL,[65] with an energy window for saving structure of 10 kJ/mol. The algorithm used was the Monte Carlo method with MMFFs as the force field and a distance-dependent dielectric constant of 4.0. The ligand was then minimized using the conjugated gradient method until a convergence value of 0.005 kcal/Å·mol, using the same force field and dielectric constant used for the conformational search. The atomic charges of the ligand were calculated by using the ANTECHAMBER module of AMBER8 program.

Automated docking was carried out by means of the program AUTODOCK 3.0; AUTODOCK TOOLS[68] was used to identify the torsion angles in the ligands, add the solvent model, and assign partial atomic charges (Gasteiger for the ligands and Kollman for the receptors). The regions of interest used by AUTODOCK were defined by considering the residue Asp3.32 as the central group; in particular, a grid of 80, 50, and 30 points in the *x*, *y*, and *z* directions was constructed centered on the carbon CG of Asp3.32. A grid spacing of 0.375 Å and a distance-dependent function of the dielectric constant were used for the energetic map calculations. Using the Lamarckian genetic algorithm, all docked compounds were subjected to 100 runs of the AUTODOCK search, with the starting positions schematized in Figure 6, in which the default values of the other parameters were used. Cluster analysis was performed on the docked results using an rms tolerance of 1.0 Å. The selection of the right cluster for each ligand docked was performed by choosing the best-populated cluster; in all the cases this represented more than 50% of the entire population. For compounds **3**−**7**, we compared the results of the docking performed with both the starting orientations and choose the best-populated cluster between the two docking runs. The resulting complexes were submitted to the same protocol of molecular dynamics previously described. An analysis of the side chains position showed no considerable changes in their conformations, except for the Trp6.48 in the D2DAR and D4DAR complexes with compounds **5**−**7**, and in the D4DAR−**2** complex.

All graphic manipulations and visualizations were performed by means of the programs Maestro[65] and WebLabViewer.[69]

Acknowledgment. This work was supported by PRIN and University of Pisa.

References

(1) Brozoski, T. J.; Brown R. M.; Rosvold, H. E.; Goldman, P. S. Cognitive deficit caused by regional depletion of dopamine in prefrontal cortex of rhesus monkey. *Science* **1979**, *205*, 929−932.
(2) Spanagel, R.; Weiss, F. The dopamine hypothesis of reward: Past and current status. *Trends Neurosci.* **1999**, *22* (11), 521−527.
(3) Masaguer, C. F.; Raviña, E.; Fontenla, J. A.; Brea, J.; Tristán, H.; Loza, M. I. Butyrophenone analogues in the carbazole series as potential atypical antipsychotics: Synthesis and determination of affinities at D2, 5-HT2A, 5-HT2B and 5-HT2C receptors. *Eur. J. Med. Chem.* **2000**, *35*, 83−95.
(4) Kebabian, J. W.; Calne, D. B. Multiple Receptors for Dopamine. *Nature* **1979**, *277*, 93−96.
(5) Bunzow, J. R.; van Tol, H. H. M.; Grandy, D. K.; Albert, P.; Salon, J.; Christie, M.; Machida, C. A.; Neve, K. A.; Civelli, O. Cloning and expression of a rat D_2 dopamine receptor *c*DNA. *Nature* **1988**, *336*, 783−787.
(6) Sokoloff, P.; Giros, B.; Martres, M. P.; Bouthenet, M. L.; Schwartz, J. C. Molecular cloning and characterization of a novel dopamine receptor (D_3) as a target for neuroleptics. *Nature* **1990**, *347*, 146−150.
(7) van Tol, H. H. M.; Bunzow, J. R.; Guan, H. C.; Sunahara, R. K.; Seeman, P.; Niznik, H. B.; Civelli, O. Cloning of the gene for a human dopamine D_4 receptor with high affinity for the antipsychotic clozapine. *Nature* **1991**, *350*, 610−614.
(8) Rowley, M.; Bristow, L. J.; Hutson, P. H. Current and novel approaches to the drug treatment of schizophrenia *J. Med. Chem.* **2001**, *44*, 477−501.
(9) LaHoste, G. J.; Swanson, J. M.; Wigal, S. B.; Glabe, C.; Wigal, T.; King, N.; Kennedy, J. L. G. Dopamine D4 receptor gene polymorphism is associated with attention deficit hyperactivity disorder. *Mol. Psychiatry* **1996**, *1*, 121−124.
(10) Faraone, S. V.; Doyle, A. E.; Mick, E.; Biederman, J. Meta-analysis of the association between the 7-repeat allele of the dopamine D4 receptor gene and attention deficit hyperactivity disorder. *Am. J. Psychiatry* **2001**, *158*, 1052−1057.
(11) Kosten, T. R.; George, T. P.; Kosten, T. A. The potential of dopamine agonists in drug addiction. *Expert Opin. Investig. Drugs* **2002**, *4*, 491−499.
(12) Tamminga, C. A. Partial dopamine agonists in the treatment of psychosis. *J. Neural Transm.* **2002**, *109*, 411−420.
(13) Burris, K. D.; Molski, T. F.; Xu, C.; Ryan, E.; Tottori, K.; Kikuchi, T.; Yocca, F. D.; Molinoff, P. B. Aripiprazole, a novel antipsychotic, is a high-affinity partial agonist at human dopamine D2 receptors. Aripiprazole, a novel antipsychotic, is a high-affinity partial agonist at human dopamine D2 receptors. *J. Pharmacol. Exp. Ther.* **2002**, *302*, 381−389.
(14) Cervetto, L.; Demontis, G. C.; Giannaccini, G.; Longoni, B.; Macchia, B.; Macchia, M.; Martinelli, A.; Orlandini, E. *N*-*n*-Propyl-substituted 3-(dimethylphenyl)-piperidines display novel discriminative properties between dopamine receptor subtypes: Synthesis and receptor binding studies. *J. Med. Chem.* **1998**, *41*, 4933−4938.
(15) Macchia, B.; Cervetto, L.; Demontis, G. C.; Domiano, P.; Longoni, B.; Macchia, M.; Minutolo, F.; Orlandini, E.; Ortore, G.; Papi, C. Synthesis and dopaminergic properties of the two enantiomers of 3-(3,4-dimethylphenyl)-1-propylpiperidine, a potent and selective dopamine D4 receptor ligand. *Bioorg. Med. Chem. Lett.* **2001**, *11*, 223−225.
(16) Astra. Preclamol 3-PPP. *Drugs Future* **1987**, *12*, 88−89.
(17) Macchia, M.; Cervetto, L.; Demontis, G. C.; Longoni, B.; Minutolo, F.; Orlandini, E.; Ortore, G.; Papi, C.; Sbrana, A.; Macchia, B. New *N*-*n*-Propyl-substituted 3-aryl and 3-cyclohexylpiperidines as partial agonists at the D_4 dopamine receptor. *J. Med. Chem.* **2003**, *46*, 161−168.
(18) Klabunde, T.; Hessler, G. Drug design strategies for targeting G-protein-coupled receptors. *ChemBioChem* **2002**, *3*, 928−944.
(19) Palczewski, K.; Kumasaka, T.; Hori, T.; Behnke, C. A.; Motoshima, H.; Fox, B. A.; Le Trong, I.; Teller, D. C.; Okada, T.; Stenkamp, R. E.; Yamamoto, M.; Miyano, M. Crystal structure of rhodopsin: A G-protein-coupled receptor. *Science* **2000** *289*, 739−745.
(20) Varady, J.; Xihan, Wu.; Fang, X.; Min, J.; Hu, Z.; Levant, B.; Wang, S. Molecular modeling of the tree-dimensional structure of dopamine 3 (D3) subtype receptor: Discovery of novel and potent D3 ligands through a hybrid pharmacophore- and stucture-based database searching approach. *J. Med. Chem.* **2003**, *46*, 4377−4392.
(21) Boeckler, F.; Lanig, H.; Gmeiner, P. Modeling the similarity and divergence of dopamine D_2-like receptors and identification of validated ligand−receptor complexes. *J. Med. Chem.* **2005**, *48*, 694−709.
(22) Thompson, J. D.; Higgins, D. G.; Gibson, T. J. Clustal W: Improving the sensitivity of progressive multiple sequence alignment through sequence weighting, position-specific gap penalties and weight matrix choice. *Nucleic Acids Res.* **1994**, *22*, 4673−4680.
(23) McGuffin, L. J.; Bryson, K.; Jones, D. T. The PSIPRED protein structure prediction server. *Bioinformatics* **2000**, *16*, 404−405.
(24) Jones, D. T. Protein secondary structure prediction based on position-specific scoring matrices. *J. Mol. Biol.* **1999**, *292*, 195−202.
(25) van Leeuwen, D. H.; Eisenstein, J.; O'Malley, K.; MacKenzie, R. G. Characterization of a chimeric human dopamine D3/D2 receptor functionally coupled to adenylyl cyclase in Chinese hamster ovary cells. *Mol. Pharmacol.* **1995**, *48*, 344−351.
(26) Filteau, F.; Veilleux, F.; Levesque, D. Effects of reciprocal chimeras between the C-terminal portion of third intracellular loops of the human dopamine D2 and D3 receptors. *FEBS Lett.* **1999**, *447*, 251−256.
(27) Karnik, S. S.; Khorana, H. G. Assembly of functional rhodopsin requires a disulfide bond between cysteine residues 110 and 187. *J. Biol. Chem.* **1990**, *265*, 17520−17524.
(28) Sali, A.; Blundell, T. L. Comparative protein modeling by satisfaction of spatial restraints. *J. Mol. Biol.* **1993**, *234*, 779−815.
(29) Laskowski, R. A.; MacArthur, M. W.; Moss, D. S.; Thorton, J. M. PROCHECK: A program to check the stereochemical quality of protein structures. *J. Appl. Crystallogr.* **1993**, *26*, 283−291.
(30) Javitch, J. A.; Fu, D.; Chen, J.; Karlin, A. Mapping the binding-site crevice of the dopamine D2 receptor by the substituted-cysteine accessibility method. *Neuron* **1995**, *14*, 825−831.

(31) Javitch, J. A.; Fu, D.; Chen, J. Residues in the fifth membrane-spanning segment of the dopamine D2 receptor exposed in the binding-site crevice. *Biochemistry* **1995**, *34*, 16433−16439.
(32) Fu, D.; Ballesteros, J. A.; Weinstein, H.; Chen, J.; Javitch, J. A. Residues in the seventh membrane-spanning segment of the dopamine D2 receptor accessible in the binding-site crevice. *Biochemistry* **1996**, *35*, 11278−11285.
(33) Javitch, J. A.; Ballesteros, J. A.; Weinstein, H.; Chen, J. A cluster of aromatic residues in the sixth membrane-spanning segment of the dopamine D2 receptor is accessible in the binding-site crevice. *Biochemistry* **1998**, *37*, 998−1006.
(34) Javitch, J. A.; Ballesteros, J. A.; Chen, J.; Chiappa, V.; Simpson, M. M. Electrostatic and aromatic microdomains within the binding-site crevice of the D2 receptor: Contributions of the second membrane-spanning segment. *Biochemistry* **1999**, *38*, 7961−7968.
(35) Javitch, J. A.; Shi, L.; Simpson, M. M.; Chen, J.; Chiappa, V.; Visiers, I.; Weinstein, H.; Ballesteros, J. A. The fourth transmembrane segment of the dopamine D2 receptor: Accessibility in the binding-site crevice and position in the transmembrane bundle. *Biochemistry* **2000**, *39*, 12190−12199.
(36) Shi, L.; Simpson, M. M.; Ballesteros, J. A.; Javitch, J. A. The first transmembrane segment of the dopamine D2 receptor: Accessibility in the binding-site crevice and position in the transmembrane bundle. *Biochemistry* **2001**, *40*, 12339−12348.
(37) Shi, L.; Javitch, J. A. The second extracellular loop of the dopamine D_2 receptor lines the binding-site crevice. *Proc. Natl. Acad. Sci. U.S.A.* **2004**, *101*, 440−445.
(38) Javitch, J. A.; Li, X.; Kaback, J.; Karlin, A. A cysteine residue in the third membrane-spanning segment of the human dopamine D2 receptor is exposed in the binding-site crevice. *Proc. Natl. Acad. Sci. U.S.A.* **1994**, *91*, 10355−10359.
(39) Simpson, M. M.; Ballesteros, J. A.; Chiappa, V.; Chen J.; Suehiro, M.; Hartman, D. S.; Godel, T.; Snyder, L. A.; Sakmar, T. P.; Javitch, J. A. Dopamine D4/D2 receptor selectivity is determined by a divergent aromatic microdomain contained within the second, third, and seventh membrane-spanning segments. *Mol. Pharmacol.* **1999**, *56*, 1116−1126.
(40) Schetz, J. A.; Benjamin, P. S.; Sibley, D. R. Nonconserved residues in the second transmembrane-spanning domain of the D_4 dopamine receptor are molecular determinants of D_4 selective pharmacology. *Mol. Pharmacol.* **2000**, *57*, 144−152.
(41) Mansour, A.; Meng, F.; Meador-Woodruff, J. H.; Taylor, L. P.; Civelli, O.; Akil, H. Site-directed mutagenesis of the human dopamine D2 receptor *Eur. J. Pharmacol.* **1992**, *227*, 205−214.
(42) Cox, B.; Neve, K. A.; Neve, R. L.; et al. Contributions of conserved serine residues to the interaction of ligands with dopamine D2 receptors. *J. Neurochem.* **1992**, *59*, 627−635.
(43) Cho, W.; Mansour, A.; Taylor, L. P. Hydrophobic residues of the D2 dopamine receptor are important for binding and signal transduction. *J. Neurochem.* **1995**, *65*, 2105−2115.
(44) Woodward, R.; Coley, C.; Daniell, S.; Naylor, L. H.; Strange, P. G. Investigation of the role of conserved serine residues in the long form of the rat D_2 dopamine receptor using site-directed mutagenesis. *J. Neurochem.* **1996**, *66*, 394−402.
(45) Wiens, B. L.; Nelson, C. S.; Neve, K. A. Contribution of serine residues to constitutive and agonist-induced signalling via the D_{2s} dopamine receptor: Evidence for multiple, agonist-specific active conformations. *Mol. Pharmacol.* **1998**, *54*, 435−444.
(46) Coley, C.; Woodward, R.; Johansson, A. M.; Strange, P. G.; Naylor, L. H. Effect of multiple serine/alanine mutations in the transmembrane spanning region V of the D_2 dopamine receptor on ligand binding. *J. Neurochem.* **2000**, *74*, 358−366.
(47) Shi, L.; Javitch, J. A. The binding site of aminergic G proteincoupled receptors: The transmembrane segments and second extracellular loop. *Annu. Rev. Pharmacol. Toxicol.* **2002**, *42*, 437−467.
(48) Ballesteros, J. A.; Shi, L.; Javitch, J. A. Structural mimicry in G protein-coupled receptors: Implications of the high-resolution of rhodopsin for structure−function analysis of rhodopsin-like receptors. *Mol. Pharmacol.* **2001**, *60*, 1−19.
(49) Goodford, P. J. A computational procedure for determining energetically favorable binding sites on biologically important macromolecules. *J. Med. Chem.* **1985**, *28*, 849−857.
(50) Floresca, C. Z.; Schetz, J. A. Dopamine receptor microdomains involved in molecular recognition and the regulation of drug affinity and function. *J. Recept. Signal Transduct. Res.* **2004**, *24*, 207−239.
(51) Morris, G. M.; Goodsell, D. S.; Halliday, R. S.; Huey, R.; Hart, W. E.; Belew, R. K.; Olson, A. J. Automated docking using a lamarckian genetic algorithm and empirical binding free energy function. *J. Comput. Chem.* **1998**, *19*, 1639−1662.
(52) Pugsley, T. A.; Shih, Y. H.; Whetzel, S. Z.; Zoski, K.; Van Leeuwen, D.; Akunne, H.; Mackenzie, R.; Heffner, T. G.; Wustrow, D.; Wise, L. D. The discovery of PD 89211 and related compounds: Selective dopamine D4 receptor antagonists. *Prog. Neuropsychopharmacol. Biol. Psychiatry* **2002**, *26*, 219−226.
(53) Shih, Y. H.; Chung, F. Z.; Pugsley, T. A. Cloning, expression and characterization of a human dopamine $D_{4.2}$ receptor (CHO K1 cells) and various $D_{4.2}/D_{2L}$ chimeras (COS-7 cells). *Neuropsychopharmacol. Biol. Psychiatry* **1997**, *21*, 153−167.
(54) Kesten, S. R.; Heffner, T. G.; Johnson, S. J.; Pugsley, T. A.; Wright, J. L.; Wise, L. D. Design, synthesis, and evaluation of chromen-2-ones as potent and selective human dopamine D4 antagonist. *J. Med. Chem.* **1999**, *42*, 3718−3725.
(55) Patel, S.; Chapman, K. L.; Marston, D.; Hutson, P. H.; Ragan, C. I. Pharmacological and functional characterisation of dopamine D4 receptors in the rat retina. *Neuropharmacology* **2003**, *44*, 1038−1046.
(56) Lahti, R. A.; Evans, D. L.; Stratman, N. C.; Figur, L. M. Dopamine D_4 versus D_2 receptor selectivity of dopamine receptor antagonists: Possible therapeutic implications. *Eur. J. Pharmacol.* **1993**, *236*, 483−486.
(57) Kulagowski, J. J.; Broughton, H. B.; Curtis, N. R.; Mawer, I. M.; Ridgill, M. P.; Baker, R.; Emms, F.; Freedman, S. B.; Marwood, R.; Patel, S.; Patel, S.; Ragan, C. I.; Leeson, P. D. 3-[[4-(4-Chlorophenyl)-piperazin-1-yl]methyl]-1*H*-pyrrolo[2,3-*b*]pyridine: An antagonist with high affinity and selectivity for the human dopamine D4 receptor. *J. Med. Chem.* **1996**, *39*, 1941−1942.
(58) Lober, S.; Hubner, H.; Utz, W.; Gmeiner, P. Rationally based efficacy tuning of selective dopamine D4 receptor ligands leading to the complete antagonist 2-[4-(4-chlorophenyl)piperazin-1-ylmethyl]-pyrazolo[1,5-*a*]pyridine (FAUC 213). *J. Med. Chem.* **2001**, *44*, 2691−2694.
(59) Kortagere, S.; Gmeiner, P.; Weinstein, H.; Schetz, J. A. Certain 1,4-disubstituted aromatic piperidines and piperazines extreme selectivity for the dopamine D4 receptor interact with a common receptor microdomain. *Mol. Pharmacol.* **2004**, *66*, 1491−1499.
(60) Berman, H. M.; Westbrook, J.; Feng, Z.; Gilliland, G.; Bhat, T. N.; Weissig, H.; Shindyalov, I. N.; Bourne, P. E. The Protein Data Bank. *Nucleic Acids Res.* **2000**, *28*, 235−242.
(61) Gasteiger, E.; Gattiker, A.; Hoogland, C.; Ivanyi, I.; Appel, R. D.; Bairoch, A. ExPASy: The proteomics server for in-depth protein knowledge and analysis. *Nucleic Acids Res.* **2003**, *31*, 3784−3788.
(62) Ballesteros, J. A.; Weinstein, H. W. Integrated methods for the construction of three-dimensional models and computational probing of structure−function relations in G-protein coupled receptors. *Methods Neurosci.* **1995**, *25*, 366−428.
(63) Case, D. A.; Darden, T. A.; Cheatham, T. E., III; Simmerling, C. L.; Wang, J.; Duke, R. E.; Luo, R.; Merz, K. M.; Wang, B.; Pearlman, D. A.; Crowley, M.; Brozell, S.; Tsui, V.; Gohlke, H.; Mongan, J.; Hornka, V.; Cui, G.; Beroza, P.; Schafmeister, C.; Caldwell, J. W.; Ross, W. S.; Kollman, P. A. *AMBER8*; University of California: San Francisco, CA, **2003**.
(64) Ryckaert, J. P.; Ciccotti, G.; Berendsen, H. J. C. Numerical integration of the Cartesian equations of motion for a system with constraints: Molecular dynamics of *n*-alkanes. *J. Comput. Phys.* **1977**, *23*, 327−333.
(65) Macromodel ver. 8.5, Schrodinger Inc., 1999.
(66) Jakalian, A.; Jack, D. B.; Bayly, C. I. Fast, efficient generation of high-quality atomic charges. AM1-BCC model: II. Parametrization and validation. *J. Comput. Chem.* **2002**, *23*, 1623−1641.
(67) Wang, J.; Wang, W.; Kollman, P. A. Antechamber, an accessory software package for molecular mechanical calculations, *Abstr. Pap. Am. Chem. Soc.* **2001**, *222*, 135-COMP Part 1.
(68) http://www.scripps.edu/~sanner/python/adt.
(69) WebLab Viewer Pro 3.7; Accelrys Inc., San Diego, CA.

JM051046B